ORNL-3484
UC-34 – Physics
TID-4500 (27th ed.)



# TIME-OF-FLIGHT STUDIES OF ELECTRONS IN VACUUM

D. A. LaBar
J. A. Harter
R. D. Birkhoff

**OAK RIDGE NATIONAL LABORATORY**
operated by
UNION CARBIDE CORPORATION
for the
U.S. ATOMIC ENERGY COMMISSION

Printed in USA. Price: $1.25 Available from the
Office of Technical Services
U. S. Department of Commerce
Washington 25, D. C.

ORNL-3484

Contract No. W-7405-eng-26

HEALTH PHYSICS DIVISION

# TIME-OF-FLIGHT STUDIES OF ELECTRONS IN VACUUM

D. A. LaBar
J. A. Harter
R. D. Birkhoff

APRIL 1964

OAK RIDGE NATIONAL LABORATORY
Oak Ridge, Tennessee
operated by
UNION CARBIDE CORPORATION
for the
U.S. ATOMIC ENERGY COMMISSION

## ACKNOWLEDGMENTS

The authors would like to thank D. Pittman for his help with the electronic problems associated with the research. Credit is due Julia Thompson for her help in taking and evaluating data. We are indebted to J. G. Carter for his assistance with the design of the vacuum system and to C. W. Williams and J. H. Neiler for the amplifier which they supplied. An expression of gratitude is due the Oak Ridge Institute of Nuclear Studies for the fellowship that they provided one of us (D.A. LaBar) which made his participation in this research possible. The work was submitted to Vanderbilt University in partial fulfillment of the requirements for the degree, Master of Science for D. A. LaBar.

# TABLE OF CONTENTS

## LIST OF FIGURES

## ABSTRACT

An electron beam monochromator is under development utilizing a time-of-flight velocity selection technique. An avalanche transistor pulser supplies nanosecond gating pulses to the negatively biased grid of an electron gun. Electrons are accelerated from a negatively biased filament into a drift tube aligned with the earth's magnetic field. The electrons in their passage through the drift tube 0.83 meters in length spread out in energy with the more energetic getting to an aperture first. Velocity selection will be achieved by gating the electron beam in front of the aperture by either electrostatic or magnetic methods. Electrons able to pass through the aperture should be monoenergetic within 0.01 eV, and these monoenergetic electrons can then be used in investigations of electronic energy levels in solids. Characteristics of the system have been obtained using a flat collector at the aperture position. Pulses amplified by a transistorized pulse amplifier are delivered to a sampling oscilloscope and displayed on a chart recorder. With electrons of energies of 2 to 15 eV, pulse shapes and arrival times indicate energy spread of the order of 0.6 eV, as expected from the thermal energy of emission from the filament source. The square of the reciprocal of the arrival time is a linear function of electron energy.

# I. INTRODUCTION

Electron sources, such as the hot cathode of an electron gun, have an inherent energy spread which must be reduced to obtain the monoenergetic electron beam necessary for studies of the energy levels in solids and gases which are less than 1 eV. Various electron optical methods have been used to get the desired monoenergetic beam, but these beams still have energy spreads of 0.05 to 0.1 eV which is too wide for many investigations. To diminish the Maxwellian thermal energy spread of the electron beam several methods have been used. Magnetic analyzers have been used to reduce the energy spread to the order of 0.5 eV, in work by Lawrence,[1] and to the order of 0.15 eV, in work reported by Nottingham.[2] Another method developed by Fox et. al.[3-5] has been termed the retarding potential difference (RPD) method. This method uses an electrode with a retarding potential, $V_R$, in front of the filament to reject the low energy electrons. By decreasing $V_R$ by a small $\Delta V_R$, the difference in effect (ion current in their study of ionization cross sections) is caused by the electrons monoenergetic to within this change in the retarding potential. $\Delta V_R$ is usually of the order of 0.1 eV.

---

[1]E. P. Lawrence, Phys. Rev. 28, 947 (1926).

[2]V. B. Nottingham, Phys. Rev. 55 203 (1939).

[3]R. E. Fox, W. M. Hickam, T. Kjeldaas, Jr., and D. J. Grove, Phys. Rev. 84, 859 (1951).

[4]R. E. Fox, W. M. Hickam, and T. Kjeldaas, Jr., Phys. Rev. 89, 555 (1953).

[5]R. E. Fox, W. M. Hickam, D. J. Grove, and T. Kjeldaas, Jr., Rev. Sci. Inst. 26, 1101 (1955).

Application of the RPD method has been made also to the measurement of molecular dissociative energies[6] where the appearance potential (the zero ion current potential) may be obtained with much higher precision than was possible by former methods. Fox et. al.[4] claimed an effective electron beam energy spread of 0.06 eV. Using the RPD method of the same laboratory, Schulz[7] stated that there was an initial spread in energy when the electrodes were freshly gold plated of 0.1 eV but that the energy spread increased to about 0.5 eV after using the system to measure the excitation of $H_2O$ ions for about 50 hours. Use was made of the RPD method by Buchel'nikova[8] to measure cross sections for the capture of slow electrons. To eliminate the effect of the cathode drop on electron energies, Buchel'nikova heated the filament with pulses and extracted electrons during the time when the current through the filament was off. The energy spread of the uncorrected electron beam, according to Buchel'nikova, was 1 eV and, after applying the RPD method, the width was reduced to 0.2 to 0.3 eV. Noting the disagreement of the reported electron beam energy spreads by different experiments using the RPD method it is felt that the 0.06 eV spread reported by Fox et. al. might be open to question.

---

[6] J. F. Burns, K-1147, Oak Ridge Gaseous Diffusion Plant, Oak Ridge, Tennessee, (1954).

[7] G. J. Schulz, J. Chem. Phys. 33, 1661 (1960).

[8] I. S. Buchel'nikova, JETP (USSR) 35, 783 (1959).

A method was devised by Schulz[9] in which an electrostatic analyzer was used to obtain a beam of electrons with an energy spread of about 0.06 eV. The beam of electrons passed through the first electrostatic analyzer for energy selection, traversed a sample of nitrogen gas, and was then analyzed for energy losses by a second electrostatic analyzer similar to the first. Another electron optical method was used by Boersch et. al.[10] in which a lens monochromator was used to select a monoenergetic electron beam and another lens monochromator to analyze the electron beam which was then detected photographically. Boersch stated that he was able to reduce the electron energy spread to 0.05 eV.

In recent research[11] on low energy electron scattering, using space-charge limited emission from a Pierce type electron gun, the energy spread of the electron beam was 0.35 eV.

The present study used a time-of-flight technique to study the spread in energy of the thermionically emitted electrons. A pulse of $10^{-9}$ seconds duration is delivered to the grid of an electron gun allowing electrons to enter a drift tube. The pulse of electrons retains the thermal energy distribution with the maximum number of electrons having a energy equal to the accelerating potential. As the electron bunch drifts down the drift tube, the electrons spread

---

[9] G. H. Schulz, Phys. Rev. 125, 229 (1962).

[10] H. Boersch, J. Geiger, and H. Hellwig, Phys. Rev. Letters, 3, 65 (1962).

[11] R. H. Neynaber, L. L. Marino, E. W. Rothe, and S. M. Trujillo, Phys. Rev. 129, 2069 (1963).

out in energy with the more energetic electrons getting ahead of the slower ones. For a specified drift distance the time-of-flight is a characteristic of the electron energy. It is proposed to activate an electrostatic or magnetic gate at the far end of the drift tube to allow a group of monoenergetic electrons to emerge where they may be used for electron energy loss studies.

Electrons with an energy of 3 eV travel with a velocity of about $10^6$ meters/second and hence take one microsecond to drift a distance of a meter. If pulses at the grid and the gate of $2 \times 10^{-9}$ seconds duration are used, then the indeterminancy in time should produce an indeterminancy in the electron energy of but 0.01 eV.

# II. APPARATUS

## A. Drift Tube

The drift tube (seen in Fig. 1) is aligned with the earth's magnetic field with the electron gun mounted on a flange at the bottom of the tube and the collector on a flange at the center. The drift tube is made from two sections of copper tubing 1.02 meters long with an inside diameter of 10.2 cm. Each section has ports on the ends and two additional ports in the sides. Vacuum pumps are attached to a horizontal section of copper tubing which is connected to the drift tube at the lower side port in the upper section. This connection is slotted so that the drift tube can be rotated around a horizontal axis to aid in aligning the drift tube with the earth's magnetic field. Rotation about a vertical axis is accomplished by rotating the entire apparatus and its wooden frame which rests on castors.

The lower section of the tube contains the electron gun mounted on the bottom flange. The collector and its associated grids and shields are mounted at the other end of this section in a side port typically 0.82 meters away. A plate on the side of the drift tube has in it an IRC fitting to connect the pulser to the grid of the electron gun. The upper section of the drift tube will be used later for analysis of the energies of electrons which have passed through gaseous or solid absorbers.

Copper was selected for the tube because of its availability, its good electrical conductivity, its good high vacuum characteristics and the fact that it is nonmagnetic. Collection of electrons on the

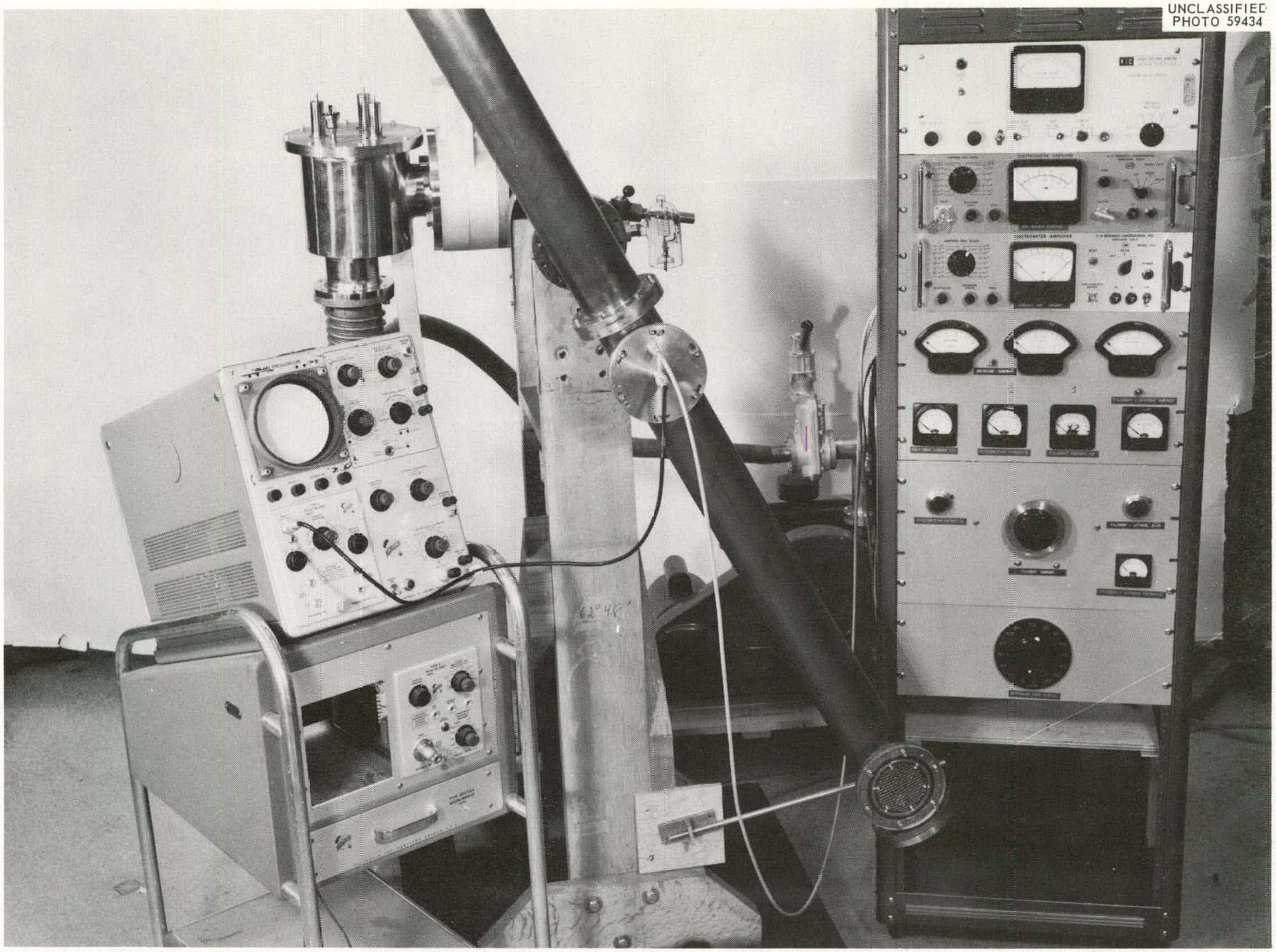


Fig. 1. Photograph of the Drift Tube, Vacuum System, and Electronic Controls.

walls of the drift tube grossly affects the paths of low energy electrons in the tube. Since metallic oxides are generally poor conductors, the inside of the tube was plated with gold. The gold plating maintains good electrical conductivity inside the drift tube. The contact potentials changed slowly as the tungsten filament evaporated to the tube and electrodes of the gun.

The selection of the correct tube diameter depended on several factors. To be able to recycle the vacuum system in as short a time as possible, the diameter had to be large enough so that there were no constrictions sufficient to seriously limit the flow of gases. Another very important consideration was that the tube had to be large enough to diminish the effects of space charge within the tube. The maximum current allowed in space charge flow[12] is

$$I_m = 38.5 \times 10^{-6} \, V^{3/2} \left(\frac{D}{L}\right)^2 \text{ amperes,} \tag{1}$$

$I_m$ is the maximum current down a tube of diameter D, length L, with an electron energy V. It was necessary to operate with a negligible space charge interaction in order to prevent energy transfer from electron to electron in the drift tube. There is an additional energy spread if the electrons spiral in the earth's magnetic field. The spiraling can be limited by including electron baffles along the drift tube but these baffles were not necessary in the tube used here with one exception. A single electron baffle was included

---

[12] J. R. Pierce, Theory and Design of Electron Beams, (D. Van Nostrand Company Inc. New York, 1954) page 151.

about 7 cm from the end of the electron gun to establish a field free region in the drift tube, and help prevent stray electrons from drifting around the electrodes and down the drift tube. Finally, the tube had to be of such a size as to allow ease in inserting the component parts into their proper positions. In line with these considerations a tube with an inside diameter of 10.2 cm was chosen. A somewhat larger diameter tube with annular electron baffles might prove advantageous to reduce electron scattering off the walls of the tube.

B. Vacuum System

The normal vacuum operating region of the electron gun monochromator was of the order of $10^{-7}$ Torr. To obtain this high vacuum a MCF oil diffusion pump with a pumping speed of 300 liters/sec was used with a 15 liters/sec Welch Duo-Seal forepump. A liquid nitrogen cold trap was used to remove condensable vapors from the system and to prevent oil from diffusing into the drift tube. The drift tube was covered with heater tape and asbestos to bake out the adsorbed gases on the chamber walls. The system was outgassed by heating it to about 300°C for the 15 hour over-night period and then allowing it to cool down again to room temperature. The vacuum seals in the system are Viton O-rings and are not affected by this bake out temperature.

A Baird-Alpert type VIC ionization gauge in the horizontal region of the vacuum system (seen in Fig. 1) was used to measure the vacuum. With the large diameter tubing and few bends in the system, the system came to equilibrium quickly, and the gauge provided a good measure of the vacuum in the drift space and electron gun region.

### C. Electron Gun Circuit

The electron gun circuit is shown in Fig. 2. A storage battery was used as a filament power supply because of its stability and low impedance. The milliammeter $I_{EM}$, records the current that returns to the filament, i.e., the total emission current. A 50Ω potentiometer across the filament is included in the circuit so that the accelerating potential, as read on the voltmeter $V_P$, can be with reference to the portion of the filament which lies geometrically just behind the hole in the grid. The accelerating potential $V_P$, is varied by using a potentiometer across part or all of an 18 volt battery. The micro-ammeter $I_{Em} - I_G$, indicates the emission current minus the grid current, i.e. the current from the filament to ground. The bias to the grid is measured by a potentiometer across an accurate 2 kΩ portion of a 12 kΩ voltage divider. A capacitor-resistor combination in the grid supply circuit supplies proper impedance matching to the 50Ω impedance of the pulser. The capacitance between grid and ground is about 11 pf and at 1,000 megacycles the capacitive reactance is only about 14.5Ω. Much of the capacitance of the grid is to the anode, and, by putting the anode 50Ω off ground, the impedance of the grid to ground was increased. This 50Ω resistor was eventially omitted however because no improvement in the pulse shape at the plane collector was noted.

The amplitude of the pulse from the pulser is 7 volts but by using a 5x or 10x attenuator the output electron pulse was much

UNCLASSIFIED
ORNL-LR-DWG 78910-R1

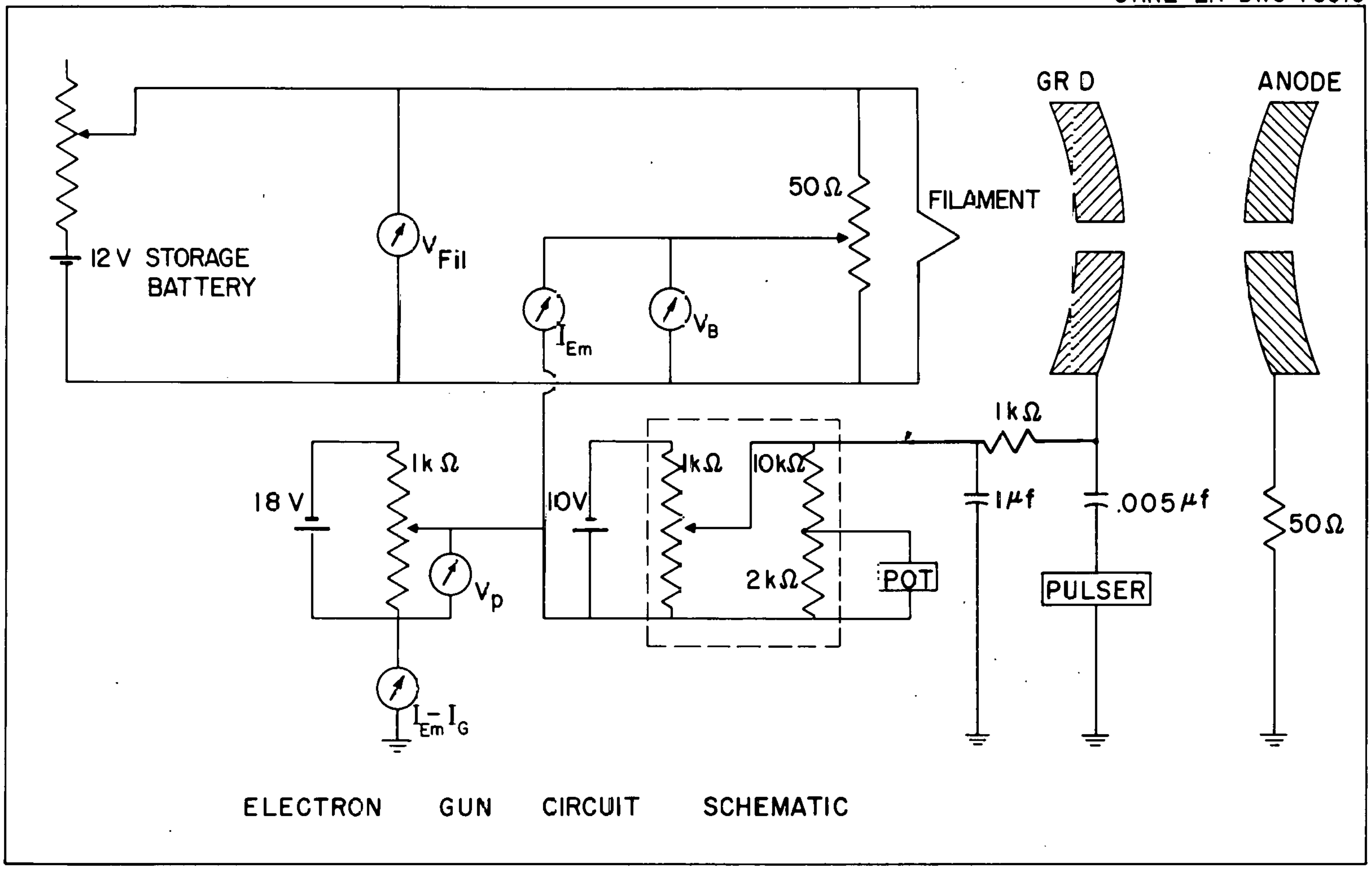


Fig. 2. Schematic Diagram of the Electron Gun Circuit.

cleaner. The data shown in this report were taken with the grid driven with a 2 or 20 nsec wide, positive pulse of either 1.4 or 0.7 volts amplitude. Later work used the full 7 volt pulse with the grid negatively biased such that it was momentarily at ground potential during the application of the pulse.

D. Electron Gun

The general form of the electron gun assembly is shown in Fig. 3. The assembly was mounted on a plate that was positioned for operation at the bottom of the drift tube. The gun assembly and plate could be removed to provide ease in changing the filament, cleaning the electrodes, etc. The filament power leads were brought out through kovars in the plate to the external battery supply.

The anode and grid were made in a similar manner with an outside diameter of 2.5 cm, a circular opening of 1.6 mm and a radius of curvature of 2.3 cm. The grid was made from nonmagnetic stainless steel because of its ability to withstand high temperatures without injury or excessive out-gassing, and the anode was made from brass. The diameter of the electrodes was chosen to prevent excessive leakage of emission current out the sides. The hole size in the electrodes was made small to have a minimum electrostatic field leakage through the holes. The back-to-back, symmetrical, curved shape arrangement was chosen to allow a minimum capacitance between the two electrodes, with the equipotential surfaces nearly parallel in the accelerating region. The spacing between the two electrodes was maintained by three equally spaced ceramic standoffs. The grid was held in place

UNCLASSIFIED
ORNL-LR-DWG 78964-R1

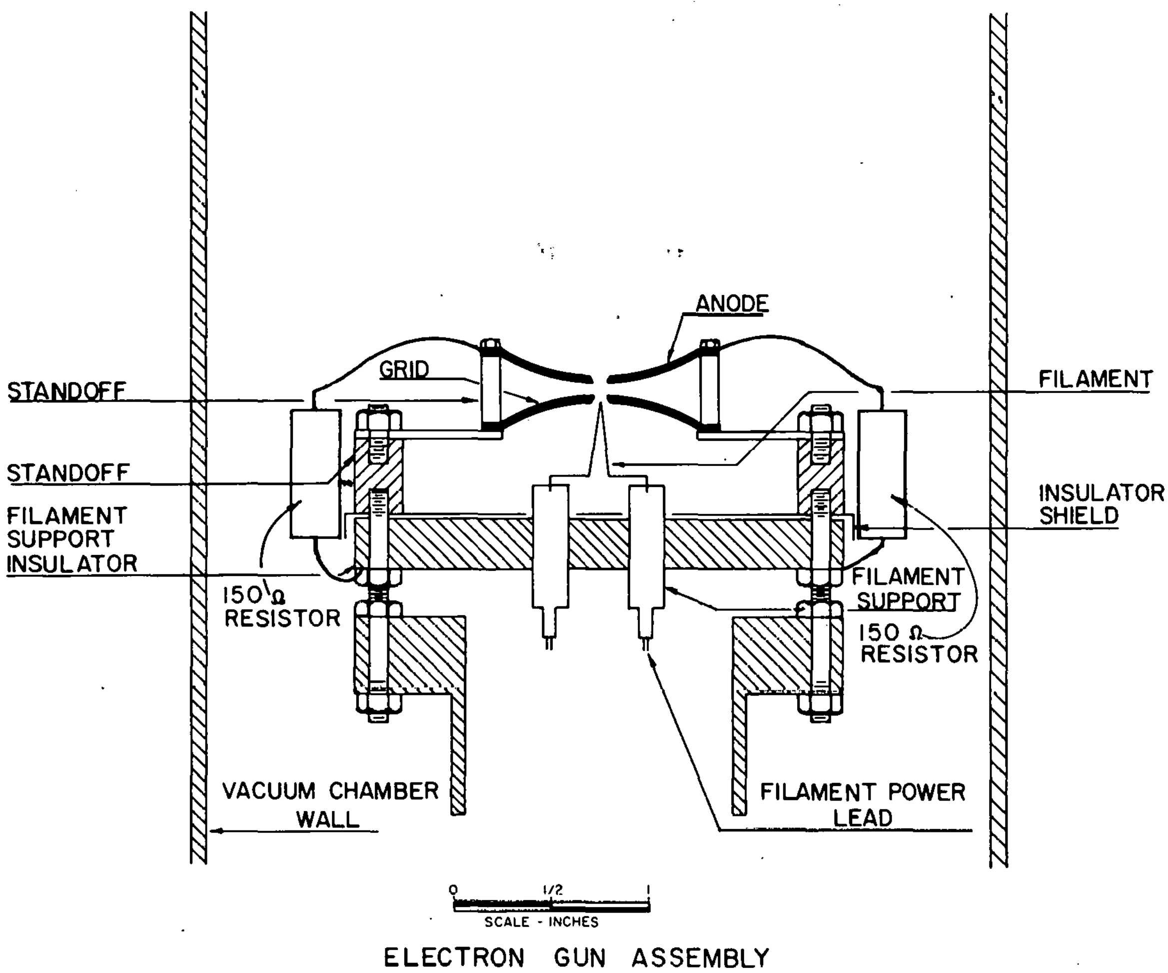


Fig. 3. Cross Sectional Drawing of the Electron Gun.

by three small bolts silver soldered to the underside of the grid which were attached to the filament support insulator by ceramic insulators. The grid to anode spacing was 2.6 mm and was kept small to provide a minimum indeterminancy in the acceleration distance.

The anode was grounded through three, 150Ω Vamistor resistors in parallel, to increase the grid to ground impedance. An insulating shield of stainless steel foil was put over the filament support insulator to prevent the insulator from collecting charge and to shield it from the electron beam. This foil was grounded through the screws that hold the insulator to the barrel of the gun. The filament supports were made of stainless steel and screwed into the lavite filament support insulator. Axial holes were drilled in the ends and fitted with set screws on the top and bottom to maintain good electrical contact with the filament and filament power leads respectively. The filament power leads were insulated from each other and from the barrel of the electron gun by ceramic beads. The ceramic insulation allowed the leads to be flexible and did not outgas as leads got hot. The pulse from the pulser was carried by a coaxial cable type RG58A/V to a coaxial kovar connection in the plate on the side of the drift tube. To minimize inductance, a leaf spring attached to the vacuum side of the kovar made contact with the underside of the grid when the gun had been positioned as desired.

The cathode was a .015" hairpin tungsten filament heated with current of from 13 to 18 amperes furnished by a 12 volt storage battery. The spread in energy of the emitted electrons by voltage drop along the filament was reduced by having most of the emission from the tip of the filament. This was done by filing down the tip to make it hotter than the rest of the filament, by providing a good heat sink for the ends of the filament into the stainless steel holders, and by bending the filament back sharply from the tip. Tungsten was chosen over other emitters since it required less care in operation, and other emitters produced no more emission. The .015" size of tungsten wire was chosen since it had a longer life than the smaller wires and still had a sufficient resistance to allow proper heating with reasonable currents. Several different filament shapes were tried but the currents emitted were about the same for each shape and, since the hairpin was the easiest to make, this type was used.

The filament was positioned about 1.6 mm from the bottom of the grid for maximum current and maximum control of the emission from the filament by the grid. The filament was operated at an emission temperature of about 2500°K to 3000°K as measured with an optical pyrometer.

## E. Avalanche Transistor Pulser

The pulse used to gate the electron gun was supplied by a Type 111 Tektronix Pretrigger Pulse Generator. This pulse generator uses an avalanche transistor in the output stage to obtain a very narrow pulse with a short rise time.

The avalanche transistor is used extensively in fast circuitry because of its very fast characteristic rise time. The bias across the junction of the transistor supplies a sufficiently high electric field so that minority carriers have enough energy to create electron hole pairs. As the voltage reaches a certain value, known as the breakdown voltage, the electrons and holes create additional pairs and they in turn multiply, etc. so that the multiplication becomes essentially infinite. The avalanche current increases very rapidly with a rise time of less than a nanosecond. The current from such a transistor is limited primarily by the external circuit resistance.[13]

In the pulse generator, a pretrigger pulse is used to initiate an internal fast ramp and trigger the sweep of a cathode ray oscilloscope. The avalanche transistor stage is triggered by a comparator stage at some point on the fast ramp. Varying the point on the fast ramp where the comparator is triggered causes a similar variation in the delay time between the pretrigger pulse and the output pulse. The avalanche transistor collector bias is set just short of the breakdown voltage and when the positive pulse from the comparator is supplied in addition to the bias, the transistor avalanches. When the avalanche transistor conducts, the collector coaxial charge line dumps its stored energy into the output circuit. A negative pulse is reflected in phase from the open end of the charge line. As this reflected pulse reaches the collector, the voltage drops sufficiently so that the transistor no longer conducts and the pulse is terminated.

---

[13]S. L. Miller and J. J. Ebers, Bell System Tech. 34, 883 (1955).

The pulse rise time is 0.5 nsec or less, and the width of the pulse can be varied from 2 nsec when only the internal charge line is used--to 142 nsec using an additional external charge line. The repetition rate can be continuously varied from 10 cps to about 100 kc maximum. For pulse widths greater than 20 nsec the repetition rate must be reduced to allow the charge line to have sufficient time to recharge and to keep from exceeding the transistor dissipation rating.

The pretrigger pulse was used to trigger the scope 30 to 250 nsec before the output pulse so that the leading edge of the output pulse could be observed.

The amplitude of the pulse output was about 7 volts positive, with negative polarity optional by using an inverting transformer. Impedance matching of the 50Ω trigger generator impedance to the grid was very important to avoid distortion of the pulse waveform. The impedance match and waveform were substantially improved by reducing the pulser output amplitude with a 5x or 10x attenuator. The grid of electron gun was pulsed with the positive 1.4 or 0.7 volt amplitude pulse that was either 2 or 20 nsec wide.

## F. Wide Bandwidth Pulse Amplifier

The signal from the electron collector was amplified before scope display by a transistorized pulse amplifier. The amplifier was developed by C. W. Williams and J. H. Neiler[14-15] with some slight modifications made to better satisfy the specific needs of the experiment. Two cascaded sections of the amplifier are designed for maximum bandwidth, and are followed by an output emitter follower, $Q_7$. Each section has an emitter follower serving as a voltage source for the feedback cascade, and uses three transistors to form a single-stage amplifier with high input and output impedance, very good frequency response, and feedback for linearity and gain stability. Each section has the following characteristics: gain = 26 db, rise time = 2.8 nsec and linear amplification of either positive or negative pulses up to 0.5 volts output.

The two stage amplifier (see Fig. 4) had the following characteristics: amplification = 430X, input capacitance = 4.7 pf, input impedance = 480Ω, and decay time of 8 nsec. In Fig. 5 the trace of the output pulse from the pulse generator is shown at the input of the amplifier and at the output. The rise time of the pulse at the input to the amplifier is 0.6 nsec and the decay time is 2 nsec. At the output of the amplifier, the rise time is 9 nsec and the decay time 8 nsec.

## G. Cathode Ray Oscilloscope

The cathode ray oscilloscope used to measure the drift time of the electrons was a Tektronix Type 661 Oscilloscope with a Type 5T1

---

[14] C. W. Williams and J. H. Neiler, IRE Trans. Nuclear Sci. NS-9, 1, (1962).

[15] C. W. Williams, private communication.

UNCLASSIFIED
ORNL – DWG. 63 – 490

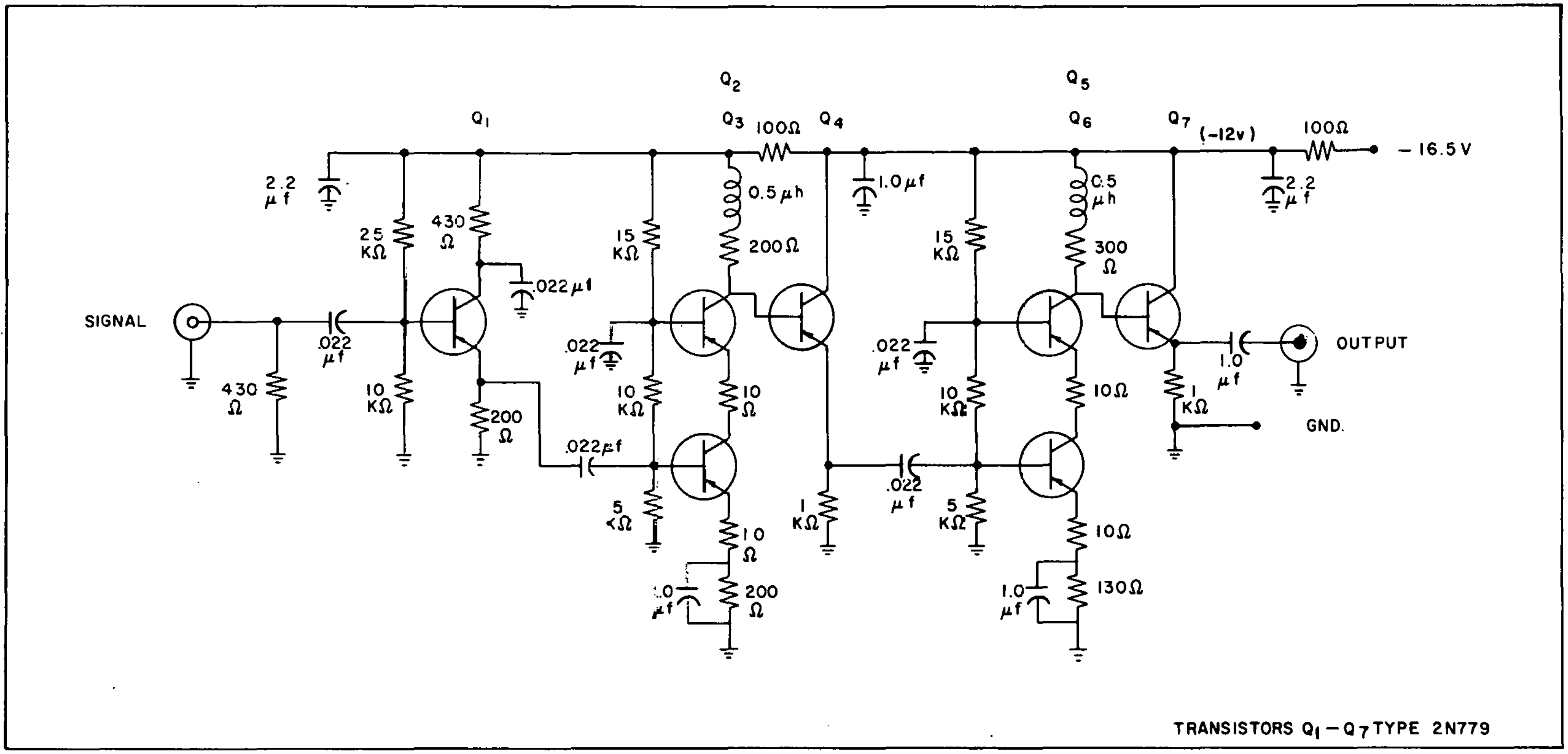


WIDE BANDWIDTH PULSE AMPLIFIER

Fig. 4. Schematic Diagram of the Transistorized Pulse Amplifier.

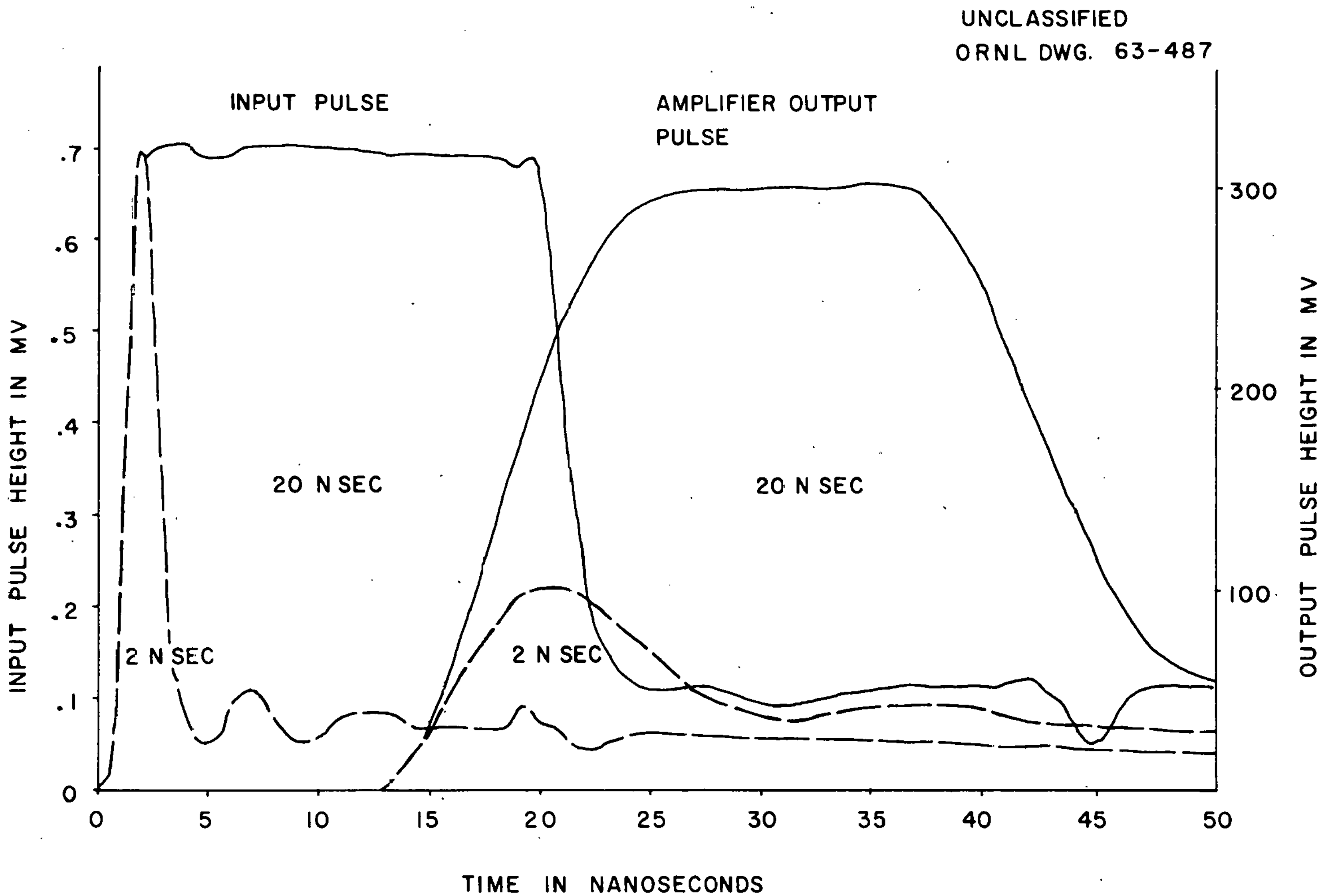


Fig. 5. Representative Input and Output Pulses to the Pulse Amplifier.

Timing Unit and a Type 4S1 Dual-Trace Sampling Unit. The rise time of such a unit is 0.35 nsec with an input impedance of 50Ω. The sweep speeds can be varied from 1 nsec/cm to 100 nsec/cm with further amplification possible by using the horizontal sweep magnifier. The scope uses a staircase sweep generator to obtain an incremental sampling of a repetitive input pulse. By taking successive samples the scope is able to reconstruct the input signal.

The oscilloscope was used as a timing device to measure the drift time of the electrons. The trace of the output pulse from the trigger generator was used as a time reference on the scope and then the difference in time between the trace of the generator pulse and the trace of current from the collector was the time-of-flight (minus, of course, the delay time in the amplifier and cables).

By using a synchronous motor to drive the manual horizontal scan of the scope at a constant speed and by delivering the vertical output signal from the scope to a chart recorder, reproduction of the scope trace was obtained. The DC offset control on the scope was adjusted to properly position the trace on the chart recorder. A fiducial mark was included on the recorder trace by depressing a push button switch as the horizontal sweep crossed each cm mark on the scope face. The recorder averaged the vertical trace on the scope for each position of the horizontal drive thus greatly reducing the random noise. The scope sweep speed was usually set at 100 nsec/cm and the sensitivity set at 2, 5 or 10 mv/cm.

# III. THEORY

## A. Thermionic Emission

Electrons are emitted with various amounts of energy from a hot filament. This thermally induced spread in the energy of the electrons is one of the inherent problems in obtaining a monoenergetic electron beam.

The Richardson-Dushman equation,

$$J = A_o T^2 e^{-\frac{e\Phi}{kT}} \tag{2}$$

gives the current density in amp/m$^2$ for electrons emitted in the forward direction from a hot planar cathode. The work function of the cathode material is denoted by $\Phi$, k is Boltzmann's constant, T is the absolute temperature and $A_o$ is a constant. Theoretically

$$A_o = \frac{4\pi mek^2}{h^3} \tag{3}$$

where m and e are the mass and charge respectively of an electron and h is Planck's constant.[16] Additional terms have been added to the Richardson-Dushman equation to indicate the variation of $\Phi$ with the temperature,[17] for electrons emitted to a cylindrical anode and for emission in the presence of an electric field (the Schottky effect).[18]

---

[16]G. P. Harnwell and J. J. Livingood, Experimental Atomic Physics, (McGraw-Hill, New York, 1933) pp 195-373.

[17]R. L. Sproull, Modern Physics: A Textbook for Engineers, (John Wiley and Sons, New York, 1956) pp 369-373.

[18]G. P. Harnwell and J. J. Livingood, op. cit. p 201-203.

The electrons have an initial energy described by a Maxwellian distribution. The emitted current density that can overcome a retarding potential $V_r$, is given by

$$J_r = J_o e^{-\frac{eV_r}{kT}} \qquad (4)$$

with $J_o$ the total emitted current density.[19] For a temperature of 3,000°K the energy spread of the half of the electrons in the center of the Maxwellian distribution, i.e. between $J_r/J_o = 1/4$ and $J_r/J_o = 3/4$, is 0.28 eV. The average energy of the electrons associated with the normal component of emission is given by 1/2 kT[20] and for a temperature of 3000°K the energy is .13 eV.

## B. Space Charge Limited Emission

For a cathode-plate potential of the order of a few volts not all of the electrons emitted by the cathode are collected by the plate. Around the cathode many of the electrons form an electron cloud that presents a potential hill to the emitted electrons. Many of the electrons that are emitted into the negative space charge cloud are unable to surmount the hill and return to the cathode. The current from space charge limited emission varies as the three-halves power of the potential applied with the value of the constant depending on the geometrical arrangement of the electrodes.

---

[19] K. R. Spangenberg, Fundamentals of Electron Devices, (McGraw-Hill, New York, 1957) p 142.

[20] K. T. Compton and I. Langmuir, Rev. Mod. Phys. 123 (1930).

The well known Child-Langmuir law gives the relationship between the current and applied potential for space charge limited plane parallel electrodes. The Poisson's equation for plane parallel electrodes is

$$\frac{d^2V}{dx^2} = -\frac{\rho}{\epsilon_o} \tag{5}$$

where $\epsilon_o$ is the permittivity of free space. From Newtonian mechanics

$$Ve = 1/2\ mv^2 \tag{6}$$

The current density J is given by

$$J = \rho v \tag{7}$$

where $\rho$ is the charge density. Eqs. (6) and (7) may be substituted into Poisson's equation and the latter integrated twice to yield the Child-Langmuir law

$$J = \frac{4\sqrt{2}\ \epsilon_o}{9} \sqrt{\frac{e}{m}} = \frac{2.33 \times 10^{-6} V^{3/2}}{x^2} \tag{8}$$

The integration constants are set equal to zero since the potential and the potential gradient are both taken to be zero at the cathode.[21]

Poisson's equation in cylindrical coordinates for an infinite cylindrical cathode and a coaxial plate is given by

$$\frac{d^2V}{dr^2} + \frac{1}{r}\frac{dV}{dr} = -\frac{\rho}{\epsilon_o} \tag{9}$$

---

[21]K. R. Spangenberg, op. cit. 454-455.

By using a method similar to that used with the parallel electrodes the current per meter length of filament is given by

$$I = \frac{8\pi\epsilon_o\sqrt{2}}{9} \sqrt{\frac{e}{m}} \frac{V^{3/2}}{r} = \frac{1.468 \times 10^{-6} V^{3/2}}{r_p} \frac{\text{amps}}{m} \qquad (10)$$

where $r_p$ is the radius of the plate. The equation is valid as shown only if $r_p > 10\ r_c$ where $r_c$ is the cathode radius.

It may be seen that the current is again proportional to the voltage to the three halves power. For three element electron tubes similar relationships hold if a fictitious voltage[22] is taken as defined by Equation 11:

$$V = \frac{V_g + DV_a}{1 + D} \qquad (11)$$

where $V_g$ and $V_a$ are the grid and anode voltages and D is the "penetration factor". The latter is defined as the ratio of the grid voltage required to reduce the emission to zero (${}^{bl}V_g$ or the black out voltage), and the anode voltage, and is a measure of the extent to which the electric field due to the anode penetrates the grid aperture to the cathode.

$$^{bl}V_g = DV_a \qquad (12)$$

For a value of $V_g$ equal to $-DV_a$, the tube cuts off. That is, when V = 0, I = 0 also. As the grid becomes less negative, V and I increase. This behavior is observed qualitatively for negative grid voltage

---

[22] W. Schottky, Arch. Electrotech 8, 1 and 299 Chapter IX(1919.)

in the electron gun employed here, but it is strongly modified as positive grid voltages by electron collection by the grid (see Section IVA).

It is interesting to note that the electrons are emitted into a cone of semi-vertical angle $\Theta$ given by

$$\Theta = \Theta_o V_d / {}^{bl}V_g \tag{13}$$

where $\Theta_o$ is the angle noted for $V_g = 0$.

## C. Electron Motion in a Magnetic Field

Electrons are emitted from the electron gun into a cone coaxial with the drift tube and the earth's magnetic field. Each electron takes a spiral path around the earth's field and is refocussed on the axis after one complete revolution. The angular frequency of this motion may be obtained by equating the centripetal acceleration and the magnetic force

$$\frac{mv^2}{r} = Bev \tag{14}$$

which yields an angular frequency, the cyclotron frequency of

$$\omega = \frac{Be}{m} \tag{15}$$

The period of this motion $\tau$ is then

$$\tau = \frac{2\pi m}{eB} \tag{16}$$

which has value of about 700 nsec in the earth's field of about 0.5 gauss. The axial velocity of electrons of energy eV is very nearly

$$v_a \sqrt{\frac{2Ve}{m}} \tag{17}$$

if $v_n^2 \ll v_a^2$ .

Now the axial distance s the electrons travel during one rotation in the magnetic field is given by

$$s = v_a \tau \tag{18}$$

or from Equations (16) and (17)

$$s = \sqrt{\frac{2Ve}{m}} \cdot \frac{2\pi m}{eB} = \frac{2\pi}{B} \sqrt{\frac{2Vm}{e}} \tag{19}$$

It is noted from Equation (19) that the focal length s varies as the square root of the energy. Electrons will also be focused if they are allowed to travel axial distances consisting of an integral multiple of focal lengths.[23]

D. Scattering of Electrons by Residual Gas

In determining the probability that an electron will collide with a gas molecule during its trajectory, the gas molecule can be considered as a sphere with radius r. The electron, with a radius $r_e$, will be intercepted by a gas molecule when the distance from the centers of the molecule and the electron are less than the sum of the radii, i.e. $r + r_e$. The cross sectional area for collision is then $\pi(r + r_e)^2$. The electron beam is attenuated by $e^{-N\pi(r + r_e)^2 s}$ in going a distance s through a gas of N molecules per unit volume. The ratio of the current at a distance s to the current when s = 0 is given by

---

[23]P. Klemperer, Electron Optics, (University Press, Cambridge, 1953)pp 77-84.

$$\frac{I}{I_o} = e^{-N\pi(R + r_e)^2 s} \tag{20}$$

The mean free path $\bar{s}$ is

$$\bar{s} = \frac{1}{N\pi(r + r_e)^2} \tag{21}$$

Now since $r \gg r_e$, $r_e$ can be neglected so that Eq. (21) becomes

$$\bar{s} = \frac{1}{N\pi r^2} \tag{22}$$

Equations (20) and (21) may be combined to yield,[24]

$$I = I_o\ e^{-s/\bar{s}}\ . \tag{23}$$

A gas at standard temperature and 760 mm of Hg pressure has 2.24 x $10^{-2}$ $m^3$/mole and 6.02 x $10^{23}$ molecules/mole. Now the number, N, of molecules per cubic meter at standard temperature and a pressure, P, in mm of Hg is given by

$$N = \frac{P(6.02 \times 10^{23} \text{ molecules/mole}).}{(760 \text{ mm of Hg})(2.24 \times 10^{-2} m^3/\text{mole})} \tag{24}$$

The mean free path, $\bar{s}$, in meters for a molecular radius, r, in meters and a pressure, P, in mm of Hg is then

$$\bar{s} = \frac{9.00 \times 10^{-24}}{Pr^2} \tag{25}$$

---

[24]R. L. Sproull, op. cit. p. 39-43.

## E. Time-of-Flight Design Parameters

Measurements of neutron energies by time-of-flight have been effected for many years. This method has found principal application in determinations of primary neutron spectra from nuclear reactions, and in measuring nuclear inelastic scattering and absorption cross sections. A large body of information exists on this time-of-flight technique[25] but little of it seems applicable to electron measurements because of the small energies involved which preclude use of nuclear counters and because of electron-gas molecule reactions and electron sensitivity to deflection by charged surfaces and space charge in the drift tube, all of which limit flight paths to less than one meter. The only important application of the neutron work appears to be in the similarity in the electronics requirements--both require fast, sensitive, broad-band amplifiers and sampling oscilloscopes.

The basic dimensions, times, and energies for the drift experiment were determined as follows. The fundamental equations involved are:

$$E = \frac{m}{2} v^2 \text{ and } s = vt \qquad (26)$$

The energy uncertainty is related to the velocity uncertainty by

$$\frac{\Delta E}{E} = 2 \frac{\Delta v}{v} \qquad (27)$$

No simple relationship exists for the uncertainties in distance and time, for these parameters are related essentially by the electron

---

[25] J. H. Neiler and W.M. Good, in Marion and Fowler's Fast Neutron Physics, (Interscience Publishers, Inc., New York, 1960), Part 1, pp 509-621.

motion during acceleration in the electron gun where the second of Equations 26 does not hold. An electron of energy between zero and one electron volts starts at some undetermined point in the space charge cloud between cathode and anode, is accelerated by an unknown electric field screened by the space charge, and may or may not emerge from the anode after falling through an unknown potential difference. Although no relationship exists between the distance uncertainty $\Delta s$ and the temporal uncertainty $\Delta t$, it is clear that the point of origin of the electrons can be unknown by no more than the cathode-plate distance, and the time of origin by the duration of the pulse on the grid. These uncertainties are essentially unrelated yet each contributes to the uncertainty in the velocity. It would seem reasonable to let each contribute the same uncertainty to the velocity; i.e. $\Delta s/s = \Delta v/v = \Delta t/t$.

The energy uncertainty desired, $\Delta E$, is 0.01 eV. The drift time required for magnetic focusing in the earth's field is $\tau = 700$ nsec (see Section C). A reasonable beam aperture in the gun was chosen as about 0.1 cm and for a minimal field leakage through the electrodes, the electrode spacing should be no less than this amount; that is $\Delta s = 0.1$ cm. With three of the eight unknowns specified in the five equations above, the other five unknowns are determined. In terms of the above specified values, the velocity is

$$v = \frac{t}{m}\frac{\Delta E}{\Delta s} = 1.23 \times 10^{8} \text{ cm/sec} \tag{28}$$

which corresponds to an energy $E = 4.31$ eV, a temporal uncertainty $\Delta t = 0.811$ nsec, and a flight distance $s = 86$ cm. The actual values used were very close to these with a pulse of width 2 nanoseconds at half maximum (and with electron emission occurring only near the peak of the pulse because of the negative grid bias), and a flight distance of 83 cm.

The velocity may be eliminated from Equation 26 to yield a convenient numerical relationship between E in eV and t in nsec.

$$E = 1.96 \times 10^{6}\ t^{-2} \tag{29}$$

F. Conversion of Time-of-Arrival Distribution to an Energy Distribution

The amplifier output gives the timc distribution of the electrons after they have traveled up the drift tube. To change the time distribution to an energy distribution a relationship between the two functions must be found. The number of electrons in the time interval between t and t + dt is defined as N(t)dt and the number of electrons in the energy interval between E and E + dE is likewise defined as $N'(E)dE$. Since the same number of electrons is involved in either case, the two can be set equal, i.e. $N(t)\ dt = N'(E)dE$ or

$$N'(E) = N(t)\,\frac{dt}{dE}\,. \tag{30}$$

But by differentiating Equations (26) we find that $dE = \frac{-\,ms^2}{t^3}$ dt or

$$\frac{dt}{dE} = \frac{-t^3}{ms^2}\,. \tag{31}$$

From Equations (30) and (31), $N'(E) = \frac{-N(t)t^3}{ms^2}$. Because the distance is constant, the number of electrons as a function of energy is then given by

$$N'(e)\ \alpha N(t)t^3 \tag{32}$$

# IV. RESULTS

## A. Direct Current Operation

The collector current, $I_p$, as a function of the grid voltage, $V_g$, with different accelerating potentials $V_p$ is shown graphically in Fig. 6. The positioning of the grid with respect to the filament has a marked effect on the control of the emission by the grid. By positioning the grid quite close to the filament (see Fig. 3) a slight change in the grid potential grossly affects the collector current.

The collector current, $I_p$, was collected by a 6.25 cm diameter cup located about 10 cm from the end of the electron gun. The current to the collector was measured by a Model 201C E-H Electrometer Amplifier.

A peak in the collector current occurred when the grid was about 1.5 volts negative. This apparently was caused by a contact potential between the electrodes and was also evident in the time-of-flight curve of Fig. 9. The amplification factor, obtained from Fig. 6, is about 11 in the normal operating region between the cut-off voltage and the $I_p$ peak.

The shape and close proximity of the grid to the filament causes the grid to collect much of the emitted current when it is positive. This was apparently the cause for the dip in the current after the rather sharp peak as grid voltage was increased. The field penetration from the plate affects the space charge around the filament less for the lower plate voltages. Apparently this is why $I_p$ is relatively independent of grid voltage for the low plate voltages but rapidly

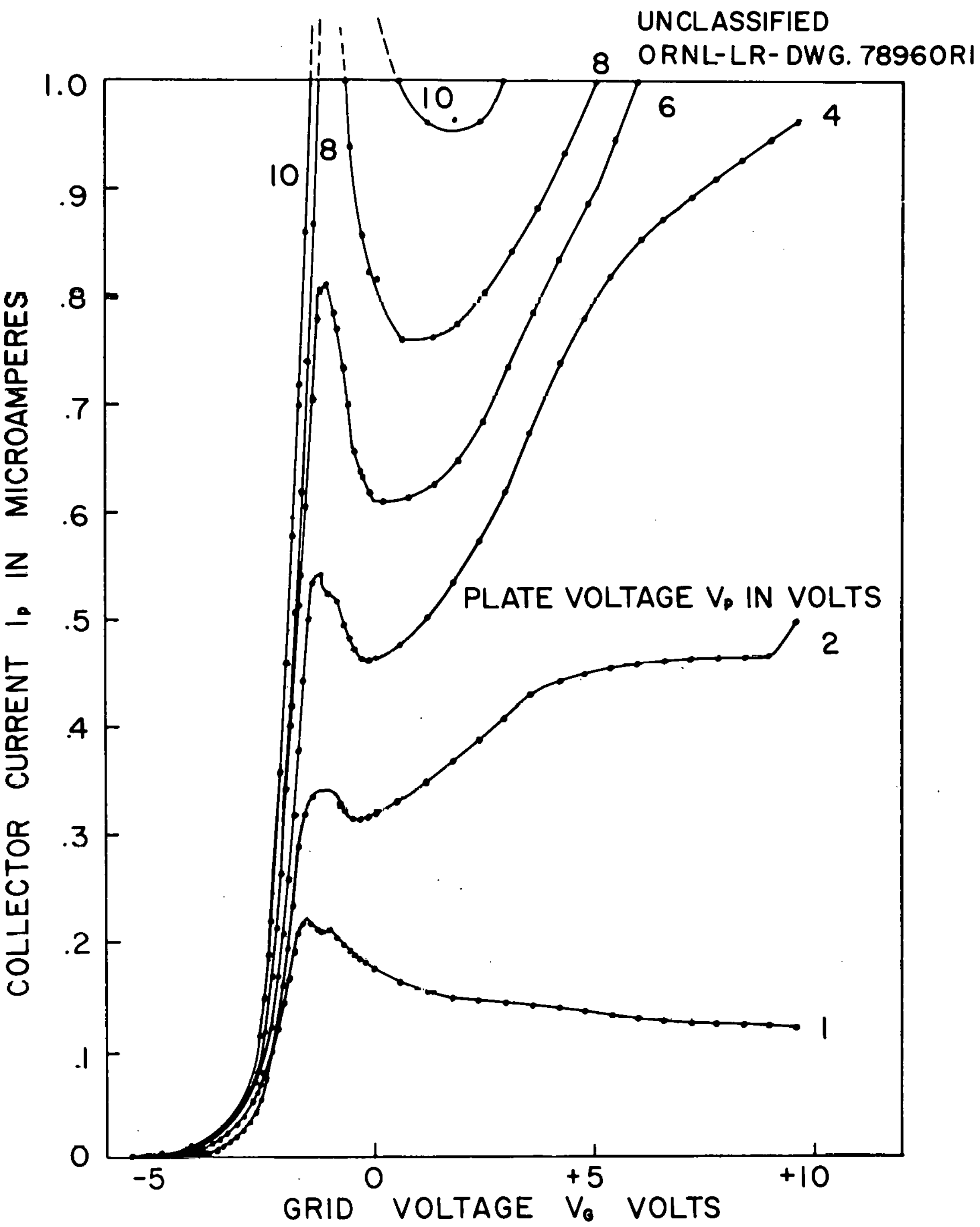


Fig. 6. Operation of Electron Gun Under Direct Current Conditions.

increases for the higher plate potentials.[26]

A grid bias of about a volt and a half below the voltage necessary for peak current diminished the collector current to 1 to 4% of its peak current value. The grid, during pulsed operation, was normally operated at 0.7 volt or more below the grid voltage necessary for peak current which kept the gun cut off until the positive pulse from the pulser was delivered to the grid.

## B. Focussing Effect of the Earth's Magnetic Field

The focussing effect of the earth's magnetic field is shown graphically in Fig. 7. To get the maximum current at the Faraday cup no baffles were placed in the drift tube. This cup was enclosed except for a 0.64 cm diameter opening to the electron beam, so that it would collect only the current arriving on the axis. The electron gun was placed at the bottom of the drift tube, and the electrons were allowed to spiral in the earth's magnetic field and be collected 84 cm away in the Faraday cup. The current collected by the cup was measured by a Model 201C E-H Electrometer.

The focal distance for electrons traveling in a uniform magnetic field varies as the square root of the electron energy as shown in Eq. 19. The electrons apparently came to a focus at the Faraday cup after having spiraled once in the earth's field in the higher energy peak, and twice in the lower energy peak. The ratio of applied voltage

---

[26] P. Klemperer, op. cit. 259-68.

UNCLASSIFIED
ORNL-LR-DWG-74875R

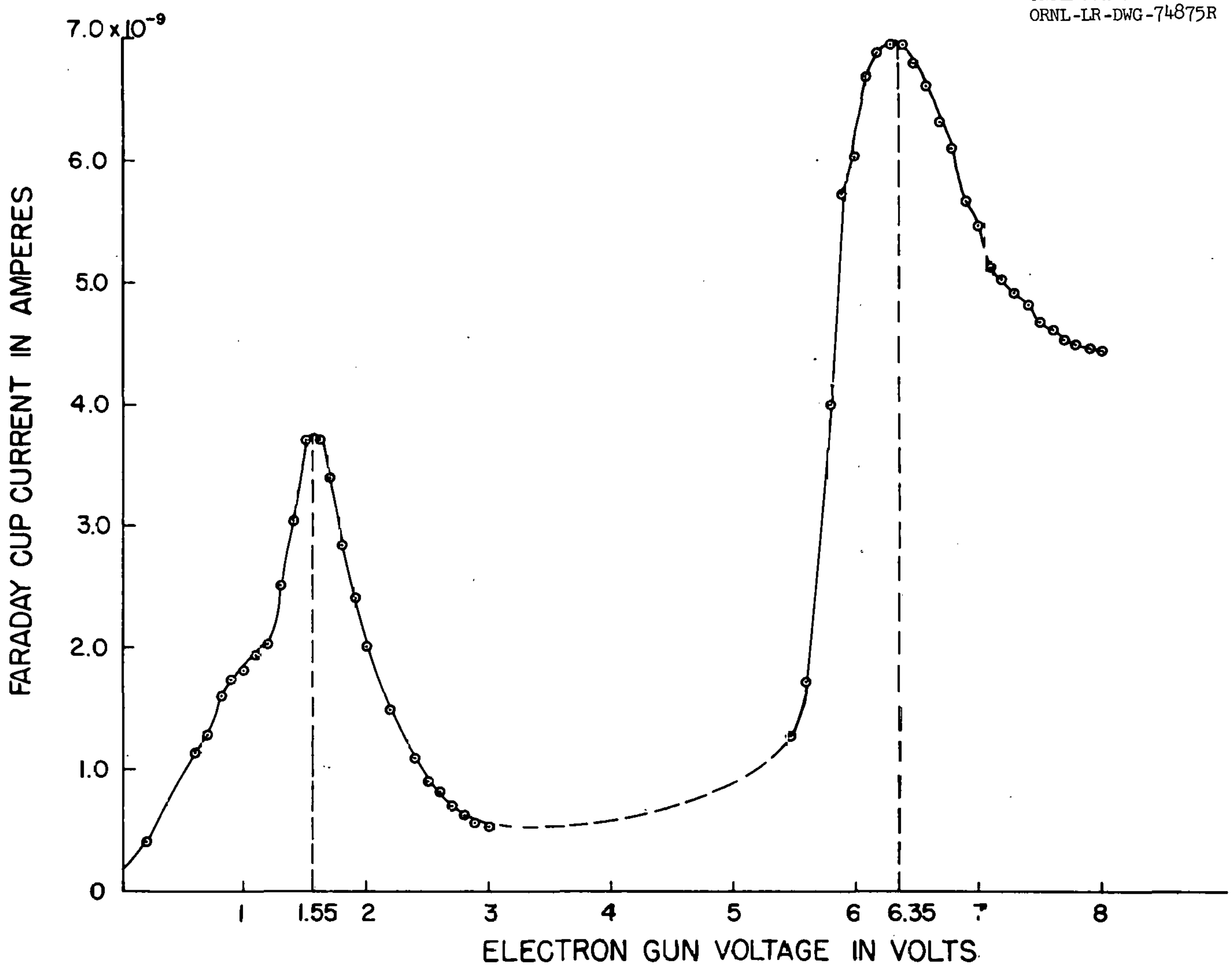


Fig. 7. Effect of the Earth's Magnetic Field on Low Energy Electrons.

for peak currents, $\frac{6.35\ V}{1.55\ V} = 4.1$, is very close to the ratio of 4 that one would expect.

The values that are obtained for the magnetic field using Equation (19) and potentials of 1.55 V and 6.35 V for the focal lengths of 1/2 s and s are 0.65 and 0.66 gauss respectively.

## C. Electron Collision Cross Sections

Electrons are absorbed or scattered for the electron beam by any residual gaseous molecules. If one takes the logarithm (to the base 10) of both sides of Equation (23) and substitutes the value of $\bar{s}$ from Equation (25) one obtains

$$\log I = \log I_o - P\left[\frac{r^2}{9 \times 10^{-24}} \log e\right] \qquad (32)$$

A plot of the log of the current vs. the pressure, as shown in Fig. 8, yields a straight line with a slope given by

$$\frac{\Delta \log I}{\Delta P} = -\frac{r^2 s \log e}{9 \times 10^{-24}} \qquad (33)$$

From the experimental slope, the molecular radius r and hence the collision cross section can then be found.

The flight path for the electrons was 83 cm, and they were collected in a Faraday cup (described in the previous section) that had an opening to the electron beam 0.64 cm in diameter. With this small aperture and the long flight path the electrons were assumed scattered out of the electron beam with a single collision. The anode voltage on the electron gun was 5.2 volts. The pressure was increased by closing a valve between the drift tube, and the pump and trap.

The collision cross section in Fig. 8 for the lower straight line is $1.34 \times 10^{-15}$ cm$^2$ and for the upper line it is $3.4 \times 10^{-15}$ cm$^2$. The first value compares reasonably well with the accepted value for the total collision cross section of $1.2 \times 10^{-15}$ cm$^2$ summarized[28] recently for molecular nitrogen.

The second value is not known with as much accuracy but is apparently larger than the most likely contaminant, water vapor, which has a cross section[29] of $1.6 \times 10^{-15}$ cm$^2$. Cross sections as high as the observed are associated with scattering off of larger molecules such as might arise from diffusion pump oil or its decomposition products. In any case, the curve was not exponential for low pressures probably due to a lack of pressure equilibrium, ion gauge pumping, or variation in ion gauge sensitivity with gas composition.

D. Drift Time Distributions

As indicated by Equation (29), there should be a linear relationship between the electron energy and the square of reciprocal time-of-flight. A plot of the square of the reciprocal time-of-flight versus the plate voltage of the electron gun is shown in Fig. 9.

The grid was operated for this measurement at 3.45 volts below the cathode potential and received a 0.7 volt positive pulse 20 nsec

---

[28] R. H. Neynaber, Lawrence L. Marion, Erhard W. Rothe, and S. M. Trujillo, "Low Energy Electron Scattering From Atomic Nitrogen", Phys. Rev. 129, 2069, (1963).

[29] H.S.W. Massey and E.H.S. Burhop, Electronic and Ionic Impact Phenomena, (Clarendon Press, Oxford, 1952) p. 208.

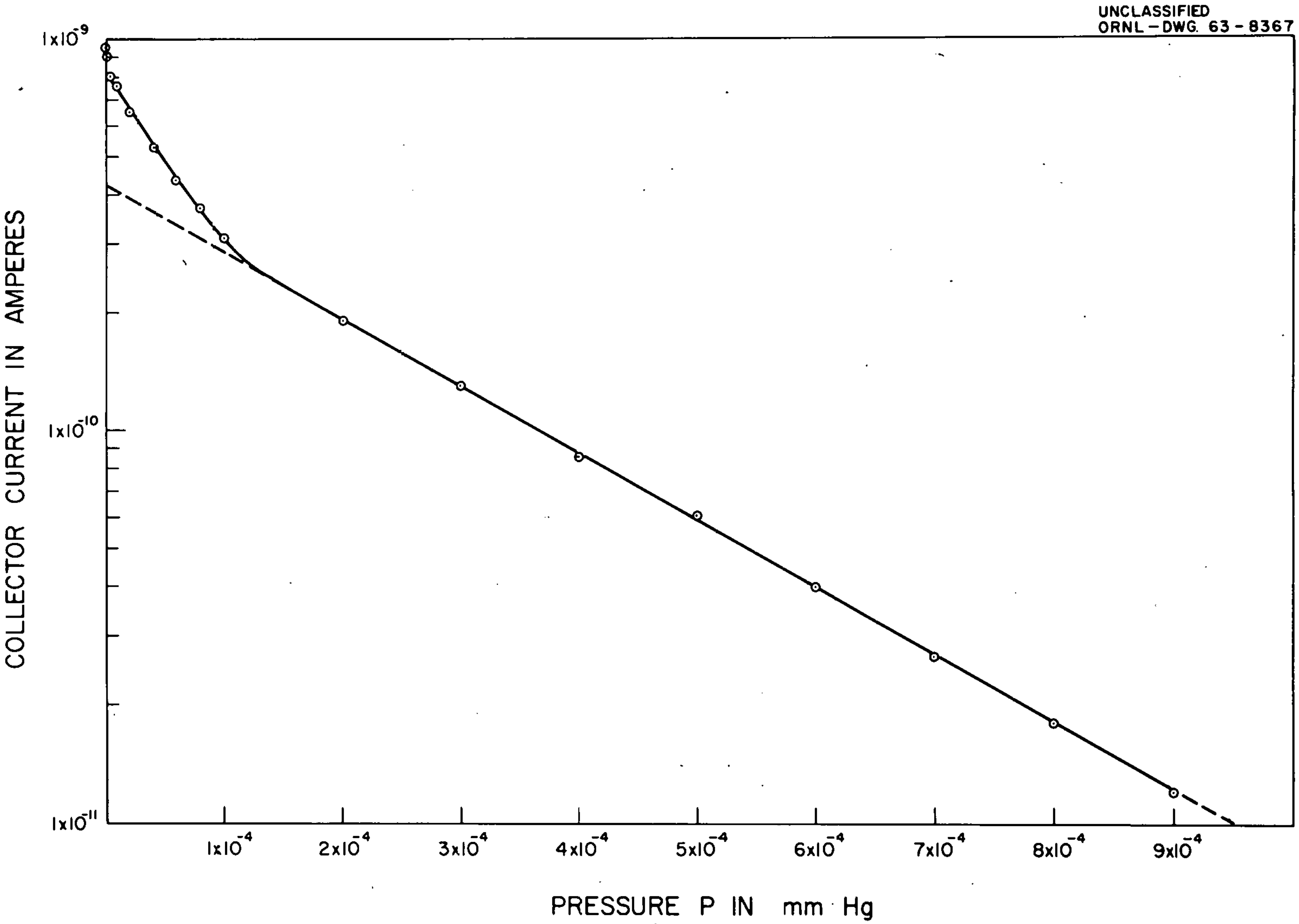


Fig. 8. Electron Collision Cross Sections with Residual Gas.

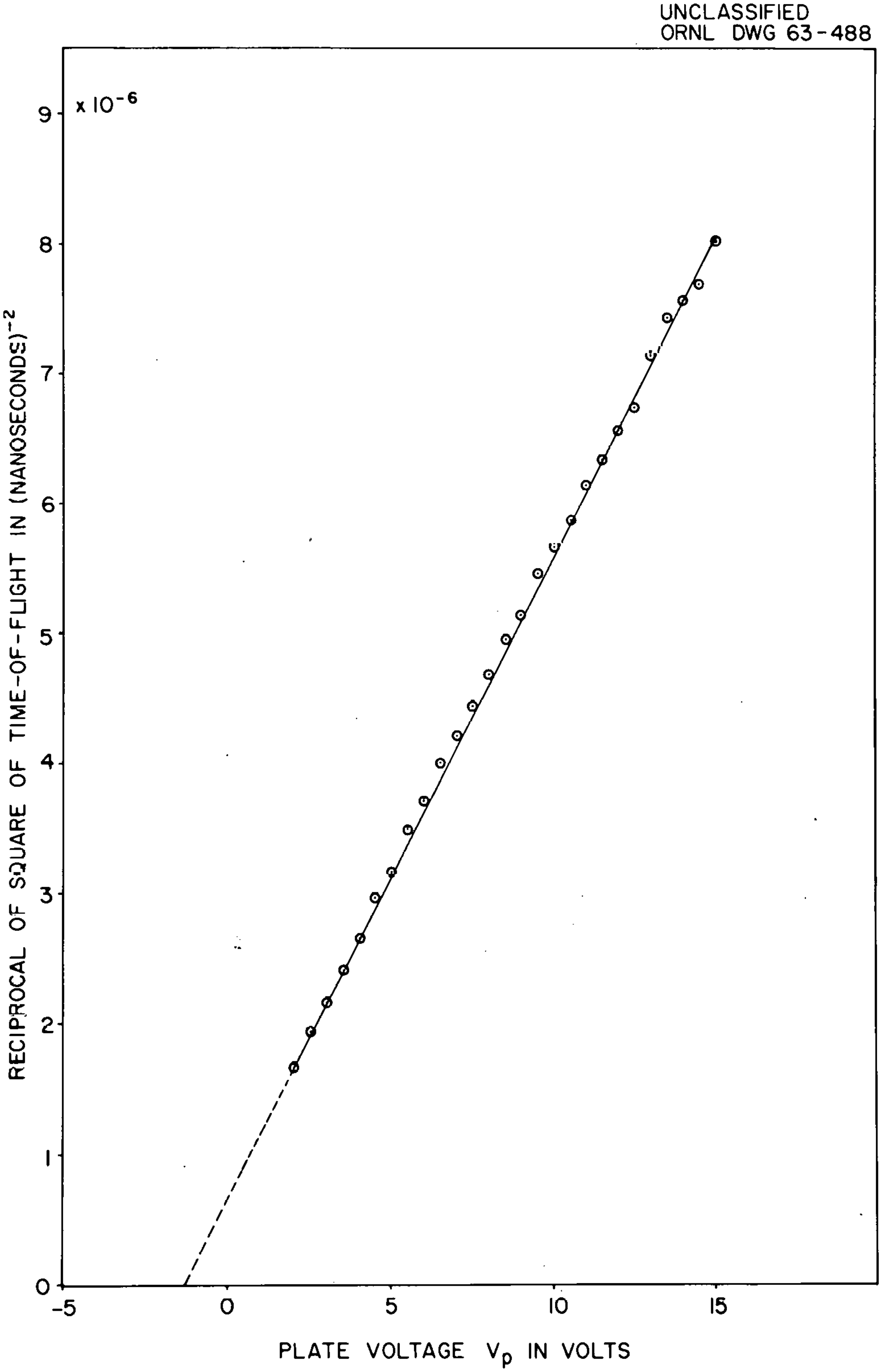


Fig. 9. Electron Gun Voltage vs. $\frac{1}{t^2}$.

in width. This pulse, used to gate the electron gun, also supplied a reference mark to the cathode ray oscilloscope. The electrons drifted down the drift tube and were collected by a plane collector 6.25 cm in diameter positioned in the drift tube a distance of 0.83 m from the electron gun. The electron pulse was amplified by the transistorized pulse amplifier and then displayed on the oscilloscope. The oscilloscope trace was reproduced on a recorder chart by feeding the oscilloscope vertical output to the recorder while driving the manual horizontal scan with a synchronous motor. Measurements were restricted to the eight centimeter linear portion of the horizontal sweep. The reference pulse was displayed on the scope trace so that the reference time could be accurately determined. A push button fiducial marker was depressed as the scan passed each cm mark on the scope face so that the position of the pulse could be accurately measured with reference of the cm-fiducal marks. The delay time in the cable and amplifier of 16 nsec was subtracted from the displayed time-of-flight.

The curve of Fig. 9, extrapolated to infinite time, intercepts the energy axis at about -1.5 volts. This intercept was attributed to a contact potential in the gun. The reciprocal slope of the line is $2.03 \times 10^{-6}$ eV $nsec^2$ which, agrees well with the value in Eq. 29 of $1.96 \times 10^{-6}$.

Three representative pulses, taken from those used to plot Fig. 9, are displayed in Fig. 10. For the accelerating voltage of 7.5 volts the pulse at half height is 26 nsec wide with an appreciable portion

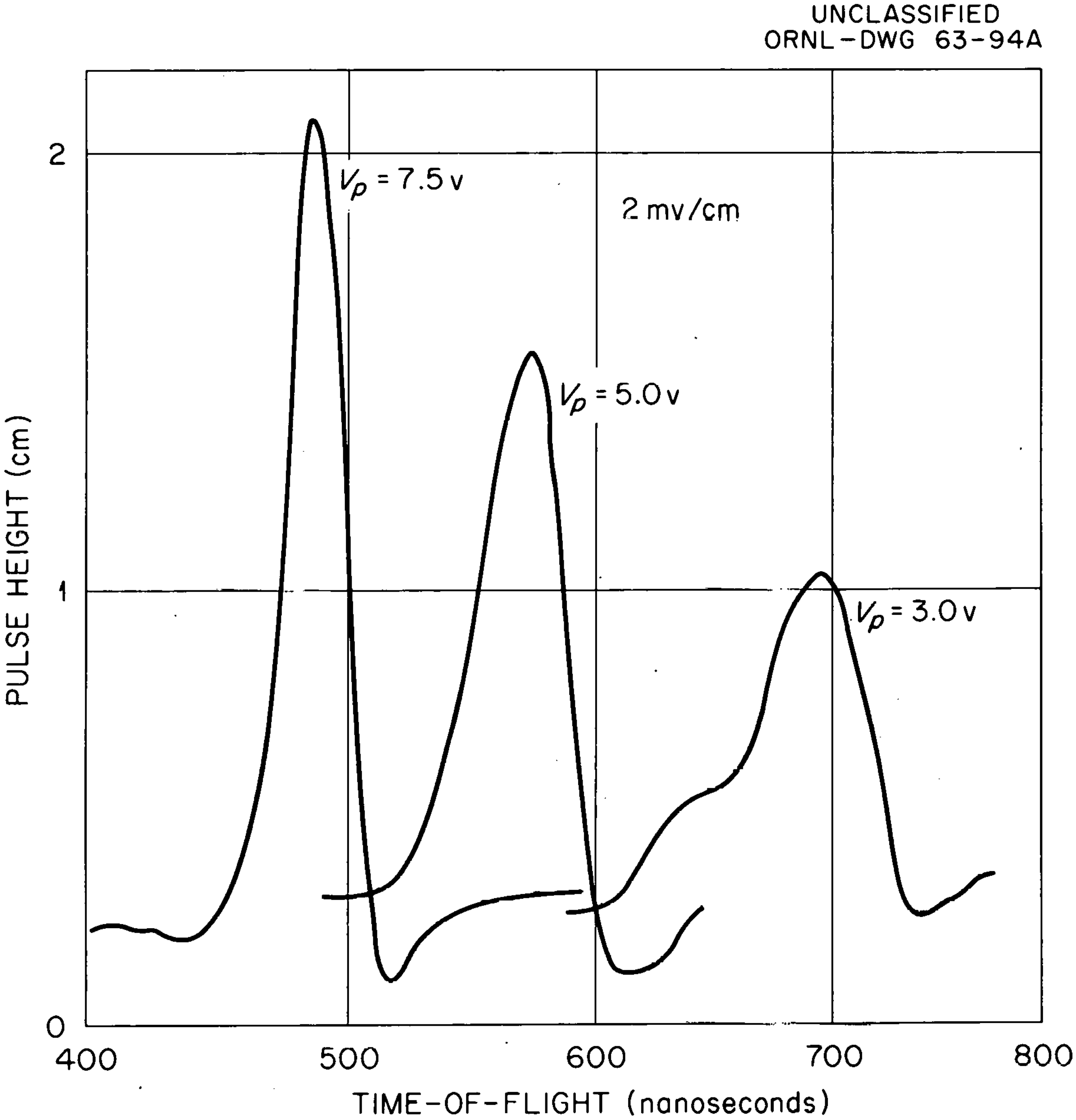


Fig. 10. Arrival Time Distribution of Pulsed Electron Beam.

of this pulse width introduced by the amplifier and the 20 nsec wide gating pulse. The width at half height for $v_p$ = 5.0 and 3.0 volts is respectively 38 and 52 nsec.

The pulses displayed in Fig. 10 were taken with the maximum amplification of the oscilloscope. The pulse generator can easily deliver a 2 nsec wide pulse but this reduces the pulse amplitude by about a factor of 10 which in turn diminishes the pulse amplitude for the low accelerating potentials to the point that it is difficult to determine the time-of-flight.

The pulses shown in Fig. 10 were divided into strips 5 nsec wide. The height of each strip, N(t), was multiplied by $t^3$ and the resulting energy distribution was plotted against the electron energy as shown in Fig. 11.

UNCLASSIFIED
ORNL-DWG-63-489

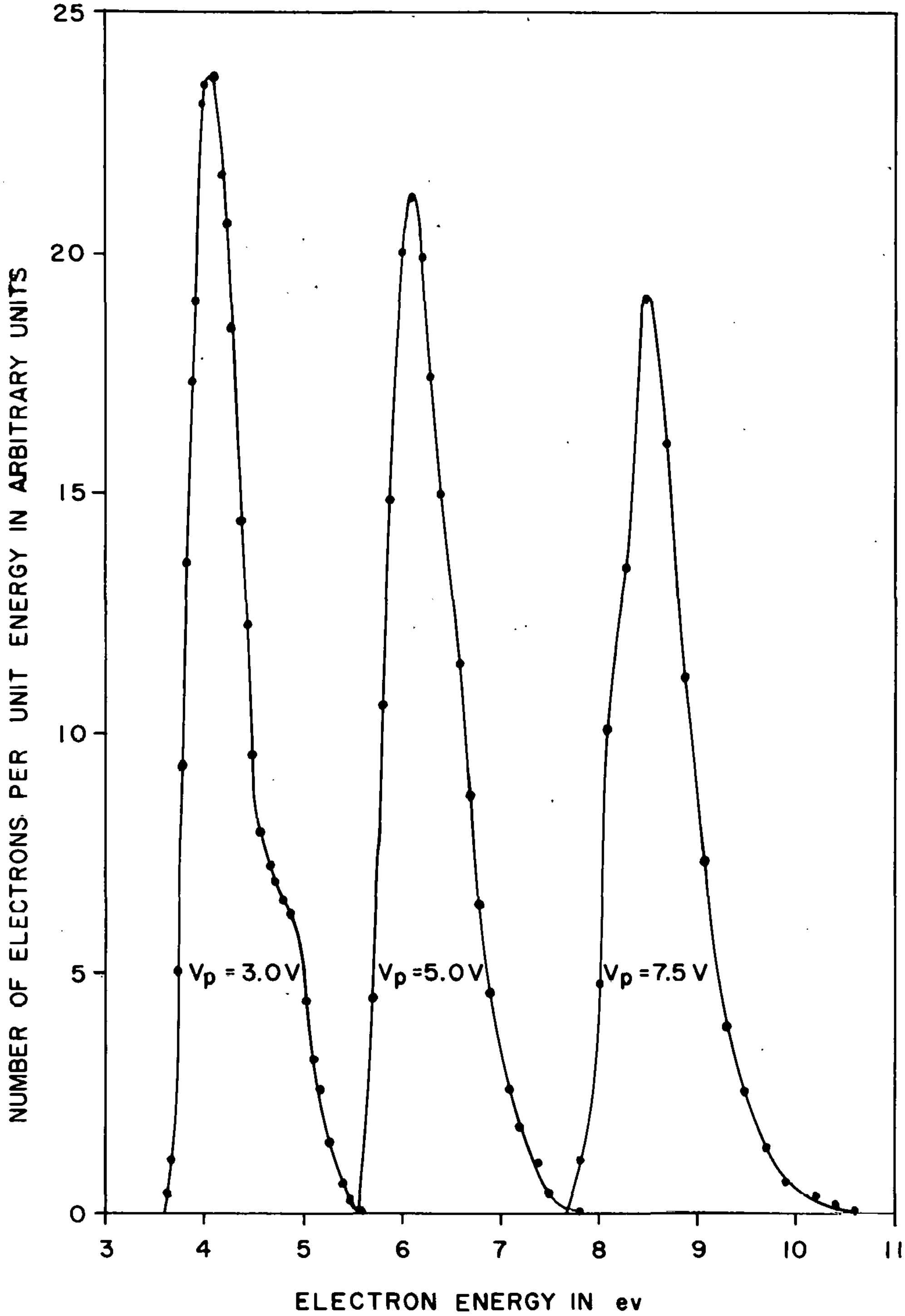


Fig. 11. Energy Distributions of Pulsed Electron Beam.

# V. CONCLUSIONS

An electron gun, drift tube, and fast amplifier have been designed and tested as a part of a time-of-flight electron beam monochromator. Drift time distributions were obtained for electrons of mean energy from 3 to 15 eV which required mean transit times from 800 to 350 nanoseconds, respectively. The widths of these distributions ranged from 52 to 24 nanoseconds, respectively, with the latter minimum value corresponding to the effects of amplifier rise time and pulse width from the pulser. The former value corresponds to an electron energy spread from the electron gun of about 0.6 eV. The reciprocal of the square of the transit time is a linear function of the electron gun accelerating potential with an intercept at -1.5 volts attributed to contact potentials. Beam attenuation due to scattering off of residual gas in the vacuum system indicated that pressures below $10^{-6}$ mm Hg are required in order to avoid loss of electrons in drift distances of the order of one meter. Additional work is required to reduce the amplifier rise time and to improve the electron gun both in regard to magnitude of emission and pulse shape at the grid. If these can be accomplished satisfactorily, then problems of gating the beam at the exit end of the tube can be studied.

BIBLIOGRAPHY

Boersch, J., Geiger, J., and Hellwig, H., "Steigerung Der Afulosung Bei Der Elecktronen-Energienanalyse," Phys. Letters 3, 64 (1962).

Buchel'nikova, I. S., "Cross Sections for the Capture of Slow Electrons by $O_2$ and $H_2O$ Molecules and Molecules of Halogen Compounds," JETP (USSR) 35, 783 (1959).

Burns, J. F., Oak Ridge Gaseous Diffusion Plant, Report K-1147, (1954) (Unpublished).

Fox, R. E., Hickam, W. M., Grove, D. J., and Kjeldaas, T. Jr., "Ionization in Mass Spectrometer by Monoenergetic Electrons," Rev. Sci. Instr. 26, 1101 (1955).

Fox, R. E., Hickam, W. M., and Kjeldaas, T. Jr., "Ionization Potentials and Probabilities Using a Mass Spectrometer," Phys. Rev. 84, 859 (1951).

Fox, R. E., Hickam, W. M., and Kjeldaas, T. Jr., "Ionization Probability Curves for Krypton and Zenon near Threshold," Phys. Rev. 89, 555 (1953).

Harnwell, G. P., and Livingood, J. H., Experimental Atomic Physics (McGraw-Hill Book Company Inc., New York, 1933) 195-203.

Klemperer, O., Electron Optics (Cambridge University Press, Cambridge England, 1953) 77-84 and 259-68.

Lawrence, E. P., "The Ionization of Atoms by Electron Impact," Phys. Rev. 28, (1926).

Massey, H.S.N. and Burhap, E.H.S., Electronic and Ionic Transport Phenomena (Clarendon Press, Oxford, 1952) 208.

Miller, S. L. and Ebers, J. J., "Alloyed Junction Avalanche Transistors," Bell System Tech. J. 34, 883 (1955).

Meiler, J. H., and Good, W. M., in Marion and Fowler's Fast Neutron Physics (Interscience Publishers, Inc., New York, 1960), Part I, 509-621.

Neynaber, R. H., Marino, L. L., Rothe, E. W., and Trujillo, S. M., "Low-Energy Electron Scattering from Atomic Nitrogen," Phys. Rev. 129, 2069 (1963).

Nottingham, W. B., "Ionization and Excitation in Mercury Vapor Produced by Electron Bombardment," Phys. Rev. 55, 203 (1939).

Pierce, J. R., Theory and Design of Electron Beams (D. Van Nostrand Company Inc., New York, 1954) 151.

Schulz, G. J., "Excitation and Negative Ions in $H_2O$," J. Chem. Phys. 33, 1661 (1960).

Schulz, G. J., "Vibrational Excitation of Nitrogen by Electron Impact," Phys. Rev. 125, 229 (1962).

Spangenberg, K. R., Fundamentals of Electron Devices (McGraw-Hill Book Company, Inc., New York, 1957) 142 and 454-5.

Sproull, R. L., Modern Physics: A Textbook for Engineers (John Wiley and Sons Inc., New York, 1956) 39-43 and 369-73.

Williams, C. W. and Neiler, J. H., "Design Considerations for Maximum Bandwidth in Transistorized Pulse Amplifiers," IRE Trans. Nuclear Sci. NS-9 1 (1962).

Williams, C. W., private communication.

THIS PAGE

WAS INTENTIONALLY

LEFT BLANK

ORNL-3484
UC-34 — Physics
TID-4500 (27th ed.)

INTERNAL DISTRIBUTION

1. Biology Library
2-4. Central Research Library
5. Reactor Division Library
6-7. ORNL — Y-12 Technical Library Document Reference Section
8-57. Laboratory Records Department
58. Laboratory Records, ORNL R.C.
59. E. T. Arakawa
60. J. A. Auxier
61. R. Baldock
62-71. R. D. Birkhoff
72. J. L. Blankenship
73. C. A. Burchsted
74. C. T. Butler
75. H. E. Goeller
76-85. J. A. Harter
86. H. H. Hubbell
87-91. G. S. Hurst
92. W. H. Jordan
93. C. E. Larson
94. K. Z. Morgan
95. M. O. Krause
96. M. J. Skinner
97. J. A. Swartout
98. A. M. Weinberg
99. J. C. Frye (consultant)
100. G. M. Fair (consultant)
101. J. B. Hursh (consultant)
102. R. L. Platzman (consultant)
103. E. P. Odum (consultant)
104. H. O. Wyckoff (consultant)

EXTERNAL DISTRIBUTION

105. D. A. LaBar, Brooks Air Force Base, San Antonio, Texas
106. J. H. Neiler, ORTEC, Oak Ridge, Tennessee
107. J. A. Simpson, National Bureau of Standards, Washington, D.C.
108. G. J. Schulz, Westinghouse Corporation Research Laboratory, Pittsburgh, Pennsylvania
109. Jake Kastner, Argonne National Laboratory, Argonne, Illinois
110. Nathanial Barr, Division of Biology and Medicine, Washington, D.C.
111. R. W. Wood, Radiological Physics and Instrumentation Branch, Washington, D.C.
112. J. A. Lough, Division of Biology and Medicine, Washington, D.C.
113. Otto Klemperer, Department of Physics, Imperial College, University of London, London, England
114. J. W. Boog, Mount Vernon Hospital, Northwood Middlesex, England
115. H. Boersch, l. Physikalisches Institut, Technische Universitat Berlin, Direktor, Berlin-Charlottenburg 2, den
116. V. B. Bhanot, Physics Department, Panjab University, Chandigarh-3, India
117. Jacobo Rapaport, University of Chile, Box 2777, Institute of Science, Santiago, Chile
118. Research and Development Division, AEC, ORO
119-753. Given distribution as shown in TID-4500 (27th ed.) under Physics category (75 copies — OTS)